

Looking for new xanthine oxidase inhibitors: 3-Phenylcoumarins versus 2-phenylbenzofurans

Benedetta Era, Giovanna L. Delogu, Francesca Pintus, Antonella Fais, Gianluca Gatto, Eugenio Uriarte, Fernanda Borges, Amit Kumar, Maria J. Matos



PII: S0141-8130(20)33593-5

DOI: <https://doi.org/10.1016/j.ijbiomac.2020.06.152>

Reference: BIOMAC 15909

To appear in: *International Journal of Biological Macromolecules*

Received date: 21 February 2020

Revised date: 2 April 2020

Accepted date: 17 June 2020

Please cite this article as: B. Era, G.L. Delogu, F. Pintus, et al., Looking for new xanthine oxidase inhibitors: 3-Phenylcoumarins versus 2-phenylbenzofurans, *International Journal of Biological Macromolecules* (2020), <https://doi.org/10.1016/j.ijbiomac.2020.06.152>

This is a PDF file of an article that has undergone enhancements after acceptance, such as the addition of a cover page and metadata, and formatting for readability, but it is not yet the definitive version of record. This version will undergo additional copyediting, typesetting and review before it is published in its final form, but we are providing this version to give early visibility of the article. Please note that, during the production process, errors may be discovered which could affect the content, and all legal disclaimers that apply to the journal pertain.

**Looking for new xanthine oxidase inhibitors:
3-Phenylcoumarins *versus* 2-phenylbenzofurans**

Benedetta Era,^{1,#} Giovanna L. Delogu,^{1,#} Francesca Pintus,¹ Antonella Fais,¹
Gianluca Gatto,² Eugenio Uriarte,^{3,4} Fernanda Borges,⁵ Amit Kumar² and
Maria J. Matos^{3,5,*}

¹ Department of Life and Environmental Sciences, University of Cagliari,
09042 Monserrato, Cagliari, Italy

² Department of Electrical and Electronic Engineering, University of Cagliari,
09123, Via Marengo 2, Cagliari, Italy

³ Departamento de Química Orgánica, Facultade de Farmacia, Universidade
de Santiago de Compostela, 15782, Santiago de Compostela, Spain

⁴ Instituto de Ciencias Químicas Aplicadas, Universidad Autónoma de Chile,
7500912 Santiago, Chile

⁵ CIQUP/Department of Chemistry and Biochemistry, Faculty of Sciences,
University of Porto, 4169-007 Porto, Portugal

* Corresponding author: Maria J. Matos (maria.matos@fc.up.pt or
mariajoao.correiapinto@usc.es)

These authors contributed equally to this work

Abstract

Overproduction of uric acid in the body leads to hyperuricemia, which is also closely related to gout. Uric acid production can be lowered by xanthine oxidase (XO) inhibitors. Inhibition of XO has also been proposed as a mechanism for improving cardiovascular health. Therefore, the search for new efficient XO inhibitors is an interesting topic in drug discovery. 3-Phenylcoumarins and 2-phenylbenzofurans are privileged scaffolds in medicinal chemistry. Their structural similarity makes them interesting molecules for a comparative study. Methoxy and nitro substituents were introduced in both scaffolds. The current study gives some insights into the synthesis and biological activity of these molecules against this important target. For the best compound of the series, the 3-(4-methoxyphenyl)-6-nitrocoumarin (**4**), the IC_{50} value, type of inhibition, cytotoxicity on B16F10 cells and ADME theoretical properties, were determined. Docking studies were also performed in order to better understand the interactions of this molecule with the XO binding pocket. This work is a preliminary screening for further design and synthesis of new non-purineric derivatives as potential compounds involved in the inflammatory suppression, specially related to gout.

Keywords: 3-Phenylcoumarins; 2-Phenylbenzofurans; Xanthine oxidase inhibitors

1. Introduction

Xanthine oxidase (XO, EC 1.2.3.2) is a form of molybdoflavin protein that plays an important role at the end of the catabolic sequence of the purine nucleotide metabolism in humans and a few other uricotelic species [1]. It firstly catalyzes the oxidation of hypoxanthine to xanthine, and then transforms it into uric acid, which is excreted in the urine [2]. This process reduces molecular oxygen to $O_2^{\cdot-}$. Hydroxyl free radicals and hydrogen peroxide, both of which are byproducts of XO activity, can cause oxidative stress in human cells.

Overproduction or under excretion of uric acid in humans can lead to hyperuricemia and gout, which is caused by crystallization and deposition of uric acid in joints and surrounding tissue [3]. Gout is a metabolic disorder associated with abnormal amounts of uric acid in the body, which causes inflammation, gouty arthritis, and uric acid nephrolithiasis. Recent studies have indicated that asymptomatic hyperuricemia is associated or may have a causal relationship with cardiovascular diseases [4].

Allopurinol (1*H*-pyrazol[3,4-*d*]pyrimidin-4-ol, Fig. 1) is a substrate and specific potent inhibitor of XO, and has been used for gout treatment for several years [5]. Different studies have indicated that allopurinol may induce hypersensitivity syndrome and Stevens-Johnson syndrome in patients [6,7,8]. More recently, febuxostat [2-(3-cyano-4-isobutoxyphenyl)-4-methyl-1,3-thiazole-5-carboxylic acid, Fig. 1], a new non-purine XO inhibitor, has been approved for the treatment of gout in the European Union and USA [5,9]. Many side effects of febuxostat have been reported [10].

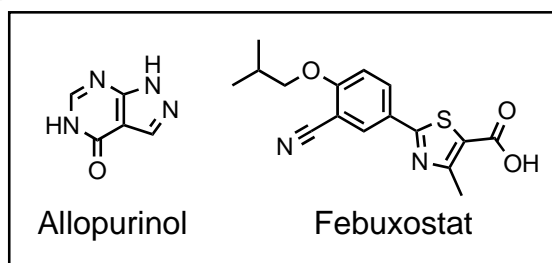


Fig. 1. Chemical structure of allopurinol (reference compound) and febuxostat.

In this study, we intended to develop XO inhibitors with potent activity and low toxicity, using compounds with a chemical structure distinct from allopurinol

and febuxostat, in order to increase the chemical spectrum of molecules acting on this target. Therefore, XO inhibitory activity of two different scaffolds was evaluated and compared with allopurinol.

2. Materials and methods

2.1. Synthesis

2.1.1. General

All reagents were purchased from Sigma-Aldrich and used without further purification. All solvents were commercially available grade. Organic solutions were dried over anhydrous Na_2SO_4 . All reactions were carried out under argon atmosphere, unless otherwise mentioned. Concentration and evaporation of the solvent after reaction or extraction was carried out on a rotary evaporator (Büchi Rotavapor) operating under reduced pressure. Reaction mixtures were purified by flash column chromatography using Silica Gel high purity grade (Merck grade 9385 pore size 60Å, 230-400 mesh particle size). Reaction mixtures were analyzed by analytical thin-layer chromatography (TLC) using plates precoated with silica gel (Merck 60 F254, 0.25 mm). Visualization was accomplished with UV light (254 nm) or potassium permanganate (KMnO_4).

2.1.2. General procedure for the preparation of 3-arylcoumarins 1-4. In a 20 mL dry Schlenk tube, to a solution of the conveniently substituted salicylaldehyde (2.46 mmol) and the arylacetic acid (2.46 mmol), in acetic anhydride (6 mL), NaH (2.46 mmol) was added in small portions, and the reaction mixture was stirred for 3 hours, at room temperature. The obtained crude was filtered and washed with diethyl ether. The obtained solid was then purified by flash chromatography (hexane/ethyl acetate 9:1) to give the desired coumarins **1-4**.

2.1.3. General procedure for the preparation of 3-arylcoumarins 5 and 6. To a 20 mL two neck round bottomed flask was added a solution of 3-chlorocoumarin (0.83 mmol), arylboronic acid (1.04 mmol), Na_2CO_3 (1.66 mmol), and Pd-salen complex (0.5 mol %), in DMF/ H_2O (1:1). The reaction mixture was heated at 110 °C for 120–180 minutes. The reaction was

monitored by chromatography. After the completion of the reaction, the mixture was extracted with ethyl acetate (3x20 mL). The organic extracts were dried over anhydrous sodium sulphate, filtrated and evaporated under vacuum. The obtained solid was purified by column chromatography (hexane/ethyl acetate 9:1) to give the coumarins **5** and **6**.

*2.1.4. General procedure for the preparation of 2-hydroxybenzylalcohols **Ia** and **Ib**.* Sodium borohydride (6.60 mmol) was added to a stirred solution of 2-hydroxybenzaldehyde (6.60 mmol), in ethanol (20 mL), in an ice bath. The reaction mixture was stirred at room temperature for 1 hour. After that, the solvent was removed, 1 N aqueous HCl solution (40 mL) was added to the residue and extracted with diethyl ether. The solvent was evaporated under vacuum to give the desired compounds **Ia** and **Ib**.

*2.1.5. General procedure for the preparation of 2-hydroxybenzyltriphenylphosphonium bromide **IIa** and **IIb**.* A mixture of 2-hydroxybenzylalcohol (16.27 mmol) and PPh₃·HBr (16.27 mmol) in CH₃CN (40 mL) was stirred under reflux for 2 hours. The obtained solid was filtered and washed with CH₃CN to give the desired compounds **IIa** and **IIb**.

*2.1.6. General procedure for the preparation of 2-phenylbenzofuran **7-12**.* A mixture of 2-hydroxybenzyltriphenylphosphonium bromide (1.11 mmol) and benzoyl chloride (1.11 mmol), in a mixed solvent (toluene 20 mL and Et₃N 0.5 mL), was stirred under reflux for 2 hours. The precipitate was removed by filtration. The filtrate was concentrated, and the residue was purified by silica gel chromatography (hexane/EtOAc 9:1) to give the desired compounds **7-12**.

2.2. Biological assays

2.2.1. XO inhibition

The biological assays were carried out following the protocol described below [11]. The reaction mixture contained 0.1 M of a phosphate buffer solution (pH 7.5), an aqueous solution of XO (0.5 U/mL, Sigma Chemical Co) and 20 µL DMSO, with or without the compound, at different doses. After mixing, a 0.82 mM of xanthine solution was added and the activity of the XO was determined

spectrophotometrically (Varian Cary 50) by measuring the formation of uric acid at 295 nm, for 5 minutes, at 37 °C. The percent of XO activity inhibition was calculated as: inhibition (%) = $(A-B)/A \times 100\%$, where A represents the difference in the absorbance of control sample between 0.5 and 1.0 minute, and B represents the difference in absorbance of the test sample between 0.5 and 1.0 minute. The IC₅₀ value, a concentration giving 50% inhibition of XO activity, was determined by interpolation of dose-response curves. Allopurinol was used as reference. All experiments were carried out three times. Continuous variables with normal distribution were presented as mean \pm SD. The final concentration containing 2% DMSO (v/v) did not affect the enzyme activity. The mode of inhibition of the enzyme was performed using the Lineweaver-Burk plot. Enzyme kinetics were determined in the absence and presence of different concentrations of the tested samples (2.5, 5.0 and 7.5 μ M), as well as different xanthine concentrations (16.6, 20, 25 and 50 μ M) as substrate.

2.2.2. Cytotoxicity

B16F10 mouse melanoma cells (CRL-6475) were purchased from the American Type Culture Collection (ATCC, Manassas, VA, USA). The cells were cultured in Dulbecco's Modified Eagle Medium (DMEM) supplemented with 10% fetal bovine serum (FBS, Gibco, NY, USA), and 1% penicillin/streptomycin at 37 °C in a humidified atmosphere with 5% CO₂. The cytotoxic effect of compound **4** was evaluated on B16F10 cells using the 3-(4,5-dimethylthiazol-2-yl)-2,5-diphenyltetrazolium bromide (MTT) assay [12]. Briefly, cells were seeded in a 96-well plate (5×10^3 cells/well) and incubated for 48 hours, at 37 °C, with the samples at different concentrations from 10 to 150 μ M. As DMSO was used to dissolve the compounds, all the activities were measured in the presence of DMSO (0.5%), as solvent control. After the incubation time, cells were labelled with MTT solution for 3 hours at 37 °C. The resulting violet formazan precipitates were dissolved in DMSO and color development was measured at 570 nm, using a microplate reader (Infinite 200, Tecan, Austria). The absorbance is proportional to the number of viable cells.

2.3. Molecular Docking

The crystal structure (PDB ID: 1FIQ) of XO [13] and the three-dimensional structure of the ligands, obtained using open babel software [14], were used for the computational study. The structure of the ligands was geometry optimized using quantum chemistry calculations [15]. The protein-ligand docking was performed using the COACH-D server [16], which predicts ligand poses by using a consensus of five methods. The final step in the protocol [17] consisted of docking the ligand into the predicted binding pockets to build their complex structures, employing the molecular docking algorithm AutoDock Vina [18]. For each predicted binding pocket, the best match to the consensus prediction of the binding residues was then selected.

3. Results and discussion

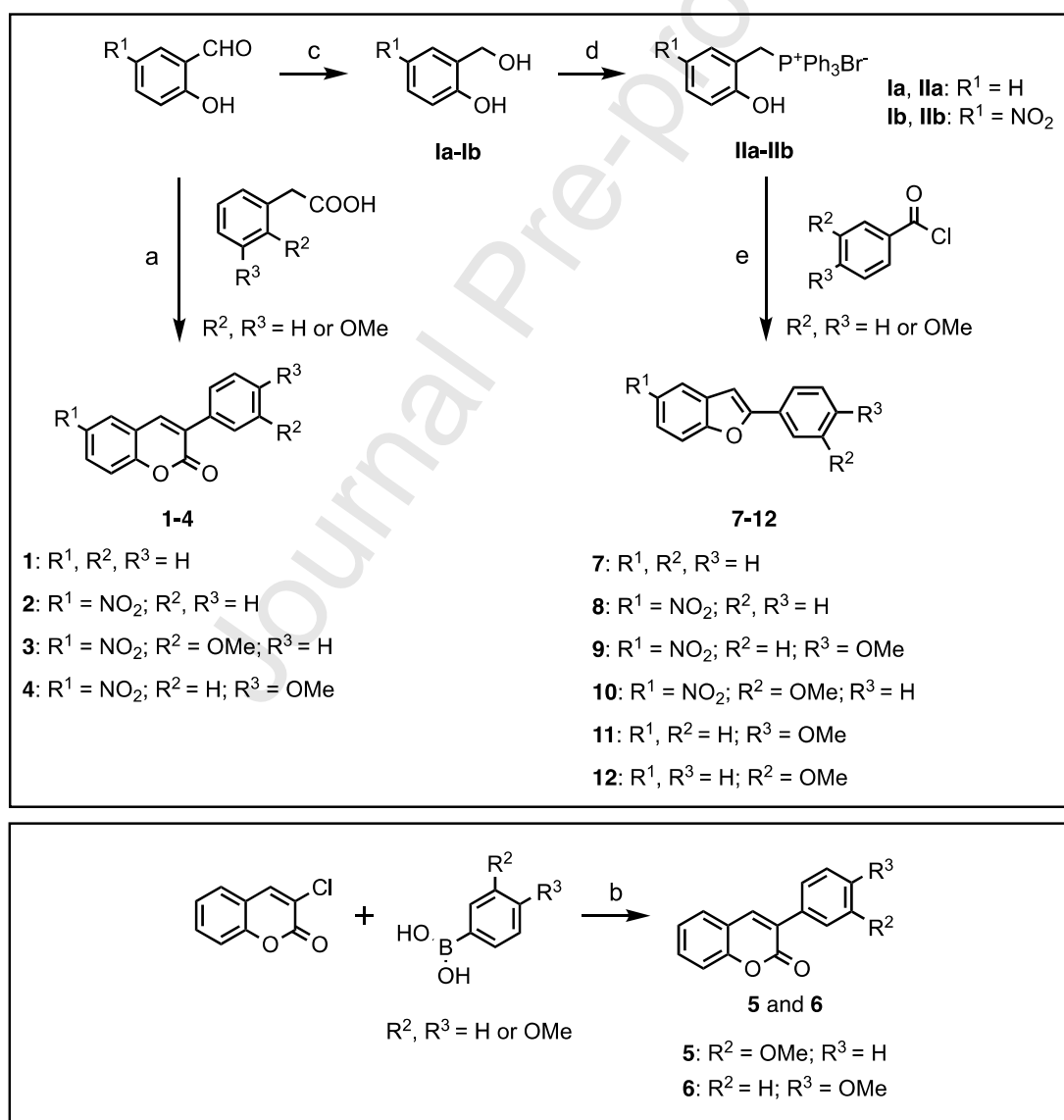
3.1. Synthesis

Based on previous findings in the field [19], and in our experience with substituted 3-phenylcoumarins and 2-phenylbenzofurans, in the present work we propose the synthesis (Scheme 1), XO inhibition evaluation (Table 1 and Fig. 2), cytotoxicity evaluation (Fig. 3) and a comparative study of a series of different substituted compounds from both families. With the aim of finding the structural features for the biological activity, we decided to explore the importance of the nature and position of small groups (methoxy and nitro substituents) into both scaffolds (Scheme 1).

The derivatives **1-4** [20,21,22] were efficiently synthesized by a condensation reaction in a dry Schlenk tube, in presence of sodium hydride and with acetic anhydride as solvent, at room temperature, for three hours. The reaction mixture was purified by flash chromatography, using hexane/ethyl acetate as eluent, in a proportion of 9:1. Starting from the commercially available salicylaldehydes and the respectively substituted arylacetic acids, we obtained four derivatives in good yields (60–75%).

The derivatives **5** [23] and **6** [23] were efficiently synthesized by a direct cross-coupling reaction, in presence of sodium carbonate (Na_2CO_3), *N,N'*-bis(salicylidene)-ethylenediamino-palladium (salen-Pd), in DMF/ H_2O (1:1), at 110 °C, for 120-180 minutes. The reaction mixture was purified by flash

chromatography, using hexane/ethyl acetate as eluent, in a proportion of 9:1. Starting from the 3-chlorocoumarin and the respectively substituted arylboronic acids, we obtained two derivatives in good yields (56 and 64%). Compounds **7-12** [24,25,26,27,28,29] were prepared via a Wittig reaction, according to the protocol outlined in Scheme 1. The desired Wittig reagents were readily prepared from the conveniently substituted 2-hydroxybenzyl alcohols **la** and **lb** and $\text{PPh}_3\cdot\text{HBr}$, in acetonitrile, at 82 °C, for two hours. The key step for the formation of the benzofuran moiety was achieved by an intramolecular reaction between the 2-hydroxybenzyltriphosponium salt **IIa** and **IIb** and the appropriate benzoyl chloride, in toluene, at 110 °C, for 2 hours, to give the six desired derivatives in good yields (40-96%).

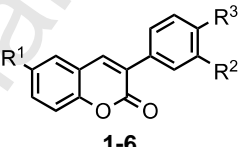


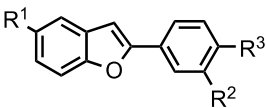
Scheme 1. Synthetic methodology to prepare compounds **1-12**. Reagents and conditions: **a)** NaH (1.0 equiv), acetic anhydride, r.t., 3 h; **b)** Na₂CO₃ (2.0 equiv), palladium complex (0.5 mol %), DMF/H₂O (1:1), 110 °C, 120-180 min; **c)** NaBH₄, EtOH, 0 °C to RT, ~2 h; **d)** PPh₃·HBr, CH₃CN, 82 °C, 2 h; **e)** toluene, Et₃N, 110 °C, 2 h.

3.2. Enzyme inhibitory studies

The inhibitory effect of compounds **1-12** on XO activity was determined spectrophotometrically by monitoring the formation of uric acid at 295 nm. Bovine milk xanthine oxidase (1332 residues), used in our enzymatic assay, is 90% homologous to human liver enzyme (1333 residues). Six 3-phenylcoumarins and six 2-phenylbenzofurans were evaluated for their ability to inhibit XO, and an overview of the effects is summarized in Table 1.

Table 1. XO inhibitory activity (% Inhibition at 100 µM and IC₅₀) of 3-phenylcoumarins, 2-phenylbenzofurans and allopurinol. Type of inhibition for compound **4** and allopurinol, the reference compound.

 1-6						
Compound	R ¹	R ²	R ³	Inhibitory activity (Inhibition % ± SD)	IC ₅₀ (µM) ± SD	Type of inhibition
1	H	H	H	75.4 ± 0.2	-	
2	NO ₂	H	H	19.2 ± 0.7	-	
3	NO ₂	OMe	H	76.6 ± 1.6	-	
4	NO ₂	H	OMe	85.1 ± 3.2	8.4 ± 1.7	uncompetitive
5	H	OMe	H	40.4 ± 4.0	-	

6	H	H	OMe	22.5 ± 1.2	-	
 <p style="text-align: center;">7-12</p>						
Compound	R ¹	R ²	R ³	Inhibitory activity (Inhibition % ± SD)	IC ₅₀ (μM) ± SD	Type of inhibition
7	H	H	H	26.3 ± 3.6	-	
8	NO ₂	H	H	*	-	
9	NO ₂	H	OMe	36.5 ± 0.9	-	
10	NO ₂	OMe	H	NI	-	
11	H	H	OMe	*	-	
12	H	OMe	H	NI	-	
Allopurinol [30]					0.1	competitive

* At 100 μM (highest concentration tested) the compounds precipitated.

NI = No inhibition observed at 100 μM.

3-(4-Methoxyphenyl)-6-nitrocoumarin (**4**) proved to be the best candidate of the series. Therefore, the IC₅₀ of this compound was calculated (IC₅₀ = 8.4 μM, Table 1). A kinetic study of this compound was also performed to understand the mechanism of enzymatic inhibition. The inhibitory binding mode was studied by using Lineweaver-Burk double reciprocal plots and the results are presented in Fig. 2. Analyzing the chart, plots of 1/V *versus* 1/[S] gave a family of parallel lines for increasing concentration. This behavior indicates that compound **4** interacts with the enzyme in an uncompetitive way. The type of inhibition is different to the reference compound, allopurinol (Table 1).

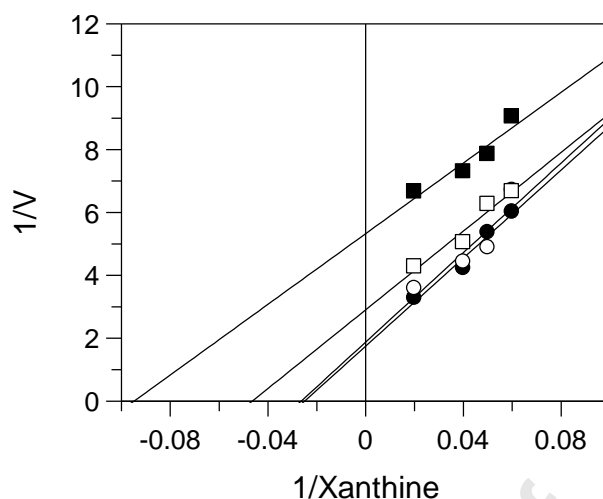


Fig. 2. Lineweaver-Burk plots for the XO inhibition caused by compound **4**. Concentrations of compound **4** were 0 (●), 2.5 (○), 5.0 (□) and 7.5 (■) μM .

3.3. Cytotoxicity assay analysis

After obtaining encouraging results from the previous experiments, biosafety effectiveness of the promising compound **4** was further evaluated, and the results represented in Fig. 3.

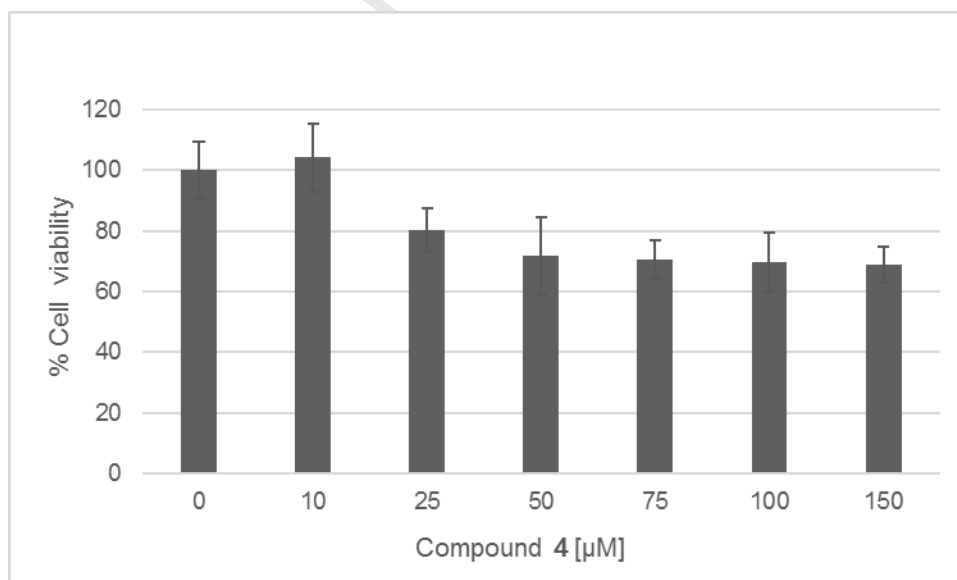


Fig. 3. The effect of compound **4** on B16F10 cell viability. Cells were treated with different concentrations of compound **4** (10-150 μM) and their viability was evaluated by MTT assay.

The results obtained support the fact that compound **4** is non-cytotoxic on B16F10 cells at the concentration in which the XO activity is inhibited (IC_{50} = 8.4 μ M).

3.4. Molecular and physicochemical properties of compounds

To better correlate the drug-like properties of the best compound (**4**), theoretical calculations were performed. For comparison, calculations were also performed for the 2-(4-methoxyphenyl)-5-nitrobenzofuran (**10**, 2-phenylbenzofuran with same substitution pattern of **4**) and allopurinol, the reference compound. Physicochemical properties, such as lipophilicity, expressed as the octanol/water partition coefficient, topological polar surface area (TPSA), molar refractivity (steric factor), number of hydrogen acceptors, number of hydrogen bond donors, volume, rotatable bonds and water solubility were calculated using Swiss ADME web tool [31] and Molinspiration program [32]. TPSA is commonly used as medicinal chemistry metric for the optimization of a drug's ability to permeate cells and achieve the desired target. The obtained *in silico* results are summarized in Table 2.

Table 2. Physicochemical properties of compounds **4** and **10**, and allopurinol, used as reference.

	Compound 4	Compound 10	Allopurinol
Volume (\AA^3)	248.88	229.89	108.68
Molar Refractivity ($\text{m}^3\text{mol}^{-1}$)	83.23	76.96	34.51
Rotatable bonds	3	3	0
H-bond acceptors	5	3	3
H-bond donors	0	0	2

Polar surface area (\AA^2)	85.26	68.19	74.44
Lipophilicity (WLogP)	3.38	4.02	0.06
Water solubility	Moderate	Moderate	Very soluble
Drug likeness (Lipinski)	Yes	Yes	Yes

Subsequently, utilizing the lipophilicity and TPSA descriptors, two crucial pharmacokinetic parameters namely gastrointestinal absorption (GA) and blood-brain barrier (BBB) were predicted using the novel Brain Or IntestinaLEstimated permeation (BOILED-Egg) method (Fig. 4).

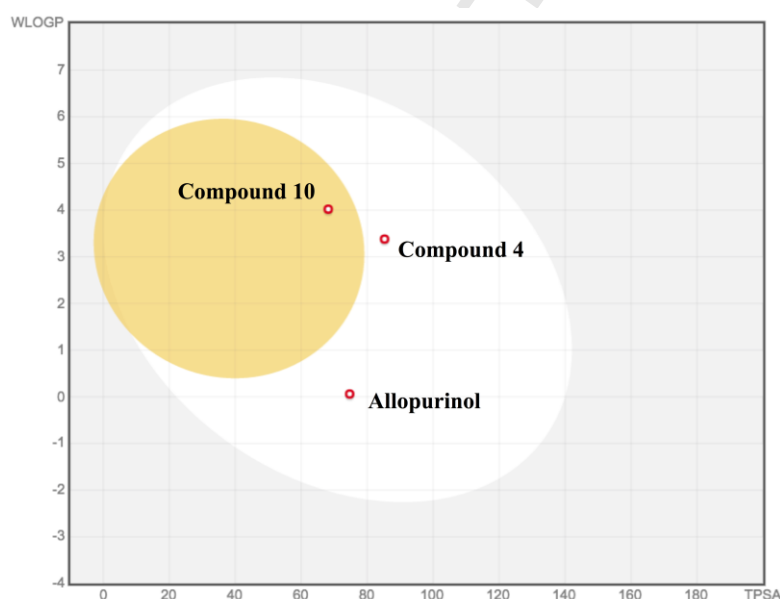


Fig. 4. BOILED-Egg construction plot for compounds **4** and **10**, and allopurinol, using WLogP and TPSA parameters. The white region represents the physicochemical space of GA and the yellow region of BBB.

It is interesting to note that the promising compound **4** and allopurinol share the physiochemical space that represents high probability of absorption in the gastrointestinal tract. Since the highest concentration of XO in humans is

present in the intestinal and liver tracts, GA is an important parameter that should be considered for the identification of lead molecules.

To better understand the uncompetitive interaction displayed by compound **4** and XO binding pocket residues, molecular docking calculations were performed for the protein-ligand complexes (Fig. 5). Since, compound **10** presents the same substitution pattern (Fig. 5C) as compound **4** (Fig. 5B), for comparison, even if compound **10** proved to be experimentally non-active, calculations were performed for both molecules.

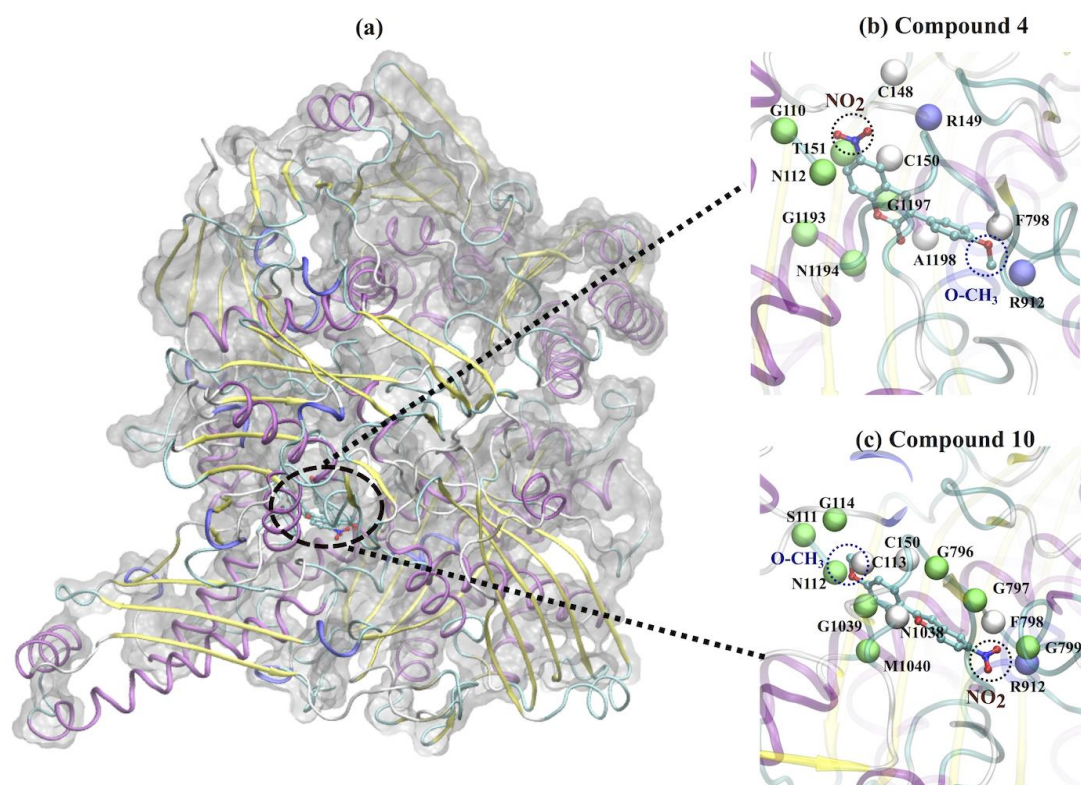


Fig. 5. Modeling XO–compound complexes. **(A)** XO protein structure shown using surface and cartoon, ligand (as licorice) and binding region highlighted with dashed circle representation. **(B)** Zoomed view of predicted ligand binding site for compound **4**. **(C)** Zoomed view of predicted ligand binding site for compound **10**.

The docking results indicated a better binding energy for compound **4** (-8.8 kcal/mol), while compound **10** displayed a lower value of -7.5 kcal/mol. The binding sites for the compounds **4** and **10**, and the amino acid residues responsible for the interactions, are shown in detail in Fig. 6.

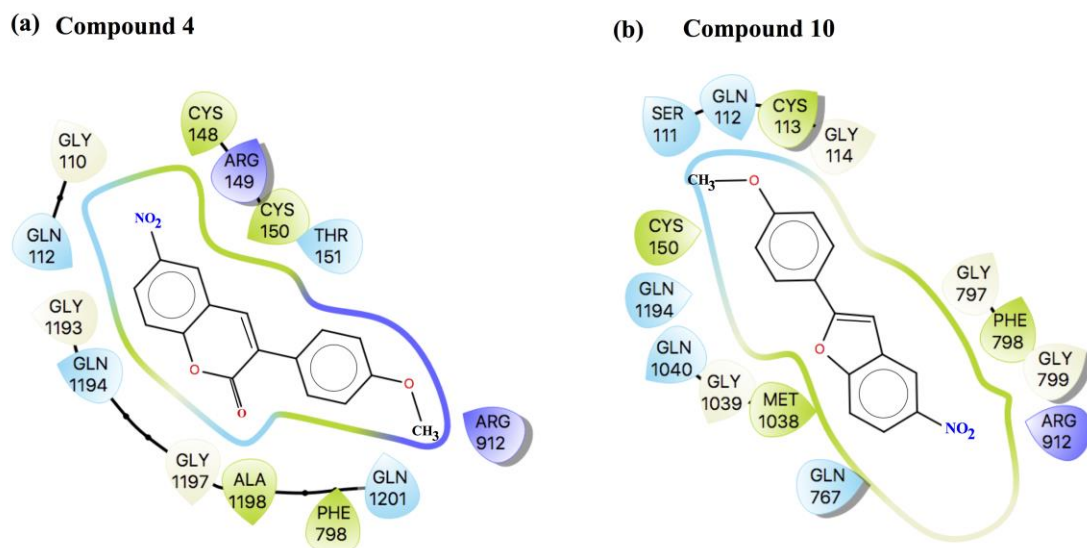


Fig. 6. Predicted docked conformation of compound **4** and **10** bound on XO binding pocket. Hydrophobic residues are in green, positive charged residues in indigo, while polar residues are represented in light blue.

The binding site for the two compounds is quite similar. However, they differ in the orientation/positioning of the methoxy group. Indeed, the orientation/positioning of methoxy group of compound **4** in the binding site facilitated additional interactions, such as π -stacking interaction (T-type) with residue Phe798, cation- π interaction and salt-bridge interaction involving the Arg912 residue. Therefore, resulting in a better docking energy with respect to compound **10**. Moreover, the residues involved in the interaction with the compounds are different from the catalytic important residues (Glu802, Arg880, Glu1261) present in the active site of XO protein, supporting the uncompetitive inhibition characteristic of compound **4**.

4. Conclusions

In summary, we investigated the XO inhibitory activity of twelve compounds, and found eight active molecules, displaying three of them inhibitory activity above 75%, at 100 μ M. All the 3-phenylcoumarins proved to be active on the studied target. The most active molecule –3-(4-methoxyphenyl)-6-nitrocoumarin (**4**)– presented an IC_{50} of 8.4 μ M against XO, inhibiting the enzyme in an uncompetitive way. Our results highlighted a relationship between the scaffold, the nature of the substituents and their position within

the scaffolds, and XO inhibitory activity. Besides being the most promising compound against the enzyme, compound **4** proved to be non-cytotoxic on B16F10 cells at the concentration in which XO activity is inhibited (~10 μ M). Also, this molecule presents pharmacokinetics and drug-likeness characteristics that support it as a promising candidate for designing effective non-purinergic XO inhibitors.

CRedit authorship contribution statement

Benedetta Era: Conceptualization, Methodology, Investigation, Writing - review & editing, Visualization **Giovanna L. Delogu**: Methodology, Investigation, Writing - review & editing, Visualization **Francesca Pintus**: Methodology, Writing - review & editing **Antonella Fais**: Conceptualization, Investigation, Visualization, Writing - review & editing, Resources **Gianluca Gatto**: Funding acquisition, Resources **Eugenio Uriarte**: Funding acquisition, Resources **Fernanda Borges**: Funding acquisition, Supervision **Amit Kumar**: Methodology, Investigation, Writing - review & editing, Data Curation **Maria J. Matos**: Conceptualization, Methodology, Investigation, Writing - Original Draft, Visualization, Supervision.

Declaration of competing interest

The authors declare that they have no known competing financial interests or personal relationships that could have appeared to influence the work reported in this paper.

Acknowledgements

This project was partially supported by the University of Porto, University of Santiago de Compostela, Xunta de Galicia (Galician Plan of Research, Innovation and Growth 2011–2015, Plan I2C, ED481B 2014/086–0 and ED481B 2018/007) and Fundação para a Ciência e Tecnologia (FCT, CEECIND/02423/2018). The present work was partially supported by FIR (Fondo Integrativo per la Ricerca – annualità 2018), University of Cagliari. This project was partially supported by Foundation for Science and Technology (FCT), and FEDER/COMPETE (POCI-01-0145-FEDER-006980). This article is based upon work from COST Action CA15135.

References

Journal Pre-proof

CRedit authorship contribution statement

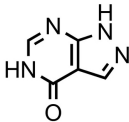
Benedetta Era: Conceptualization, Methodology, Investigation, Writing - review & editing, Visualization **Giovanna L. Delogu:** Methodology, Investigation, Writing - review & editing, Visualization **Francesca Pintus:** Methodology, Writing - review & editing **Antonella Fais:** Conceptualization, Investigation, Visualization, Writing - review & editing, Resources **Gianluca Gatto:** Funding acquisition, Resources **Eugenio Uriarte:** Funding acquisition, Resources **Fernanda Borges:** Funding acquisition, Supervision **Amit Kumar:** Methodology, Investigation, Writing - review & editing, Data Curation **Maria J. Matos:** Conceptualization, Methodology, Investigation, Writing - Original Draft, Visualization, Supervision.

-
- [1] R. Hille, Molybdenum-containing hydroxylases, *Arch. Biochem. Biophys.* 433(1) (2005) 107-116.
- [2] K. Tomovic, B.S. Ilic, Z. Smelcerovic, M. Miljkovic, D. Yancheva, M. Kojic, A.T. Mavrova, G. Kocic, A. Smelcerovic, Benzimidazole-based dual dipeptidyl peptidase-4 and xanthine oxidase inhibitors, *Chem. Biol. Interact.* 315 (2020) 1088733.
- [3] P. Richette, T. Bardin, Gout, *Lancet* 375(9711) (2010) 318-328.
- [4] E. Agabiti-Rosei, G. Grassi, Beyond gout: uric acid and cardiovascular diseases, *Curr. Med. Res. Opin.* 3 (2013) 33-39.
- [5] J.A. Singh, K.S. Akhras, A. Shiozawa, Comparative effectiveness of urate lowering with febuxostat versus allopurinol in gout: analyses from large U.S. managed care cohort, *Arthritis Res. Ther.* 17(1) (2015) 120.
- [6] B. Hammer, A. Link, A. Wagner, M. Böhm, Hypersensitivity syndrome during therapy with allopurinol in asymptomatic hyperuricemia with a fatal outcome, *Dtsch. Med. Wochenschr.* 126(47) (2001) 1331-1334.
- [7] S. Bashir, S.M. Shah, I. Babar, Allopurinol induced Stevens-Johnson syndrome: a case report, *J. Pak. Med. Assoc.* 50(6) (2000) 207-209.

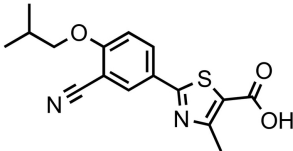
- [8] G.B. Elion, A. Kovensky, G.H. Hitchings, Metabolic studies of allopurinol, an inhibitor of xanthine oxidase, *Biochem. Pharmacol.* 15(7) (1966) 863-880.
- [9] C.L. Gray, N.E. Walters-Smith, Febuxostat for treatment of chronic gout, *Am. J. Health Syst. Pharm.* 68(5) (2011) 389-398.
- [10] B.L. Love, R. Barrons, A. Veverka, K.M. Snider, Urate-lowering therapy for gout: focus on febuxostat, *Pharmacotherapy* 30(6) (2010) 594-608.
- [11] S. Floris, A. Fais, A. Rosa, A. Piras, H. Marzouki, R. Medda, A.M. González-Paramás, A. Kumar, C. Santos-Buelga, B. Era, Phytochemical composition and the cholinesterase and xanthine oxidase inhibitory properties of seed extracts from the *Washingtonia filifera* palm fruit, *RSC Adv.* 9 (2019) 21278.
- [12] T. Mosmann, Rapid colorimetric assay for cellular growth and survival: application to proliferation and cytotoxicity assays, *J. Immunol. Methods.* 65 (1983) 55-63.
- [13] E. Cristofer, T.E. Bryan, K. Okamoto, T. Nishino, T. Nishino, E.F. Pai, *PNAS* 97(20) (2000) 10723-10728.
- [14] N.M. O'Boyle, M. Banck, C.A. James, C. Morley, T. Vandermeersch, G.R. Hutchison, Open Babel: An open chemical toolbox, *J. Cheminform.* 3 (2011) 33.
- [15] A. Kumar, G. Cappellini, F. Delogu, Electronic and optical properties of chromophores from hexeneuronic acids, *Cellulose* 26 (2019) 1489-1501.
- [16] Q. Wu, Z. Peng, Y. Zhang, J. Yang, COACH-D: improved protein-ligand binding site prediction with refined ligand-binding poses through molecular docking, *Nucleic Acids Res.* 46 (2018) W438-W442.
- [17] J. Yang, A. Roy, Y. Zhang, Protein-ligand binding site recognition using complementary binding-specific substructure comparison and sequence profile alignment, *Bioinformatics* 29(20) (2013) 2588-2595.
- [18] O. Trott, A.J. Olson, AutoDock Vina: improving the speed and accuracy of docking with a new scoring function, efficient optimization, and multithreading, *J. Comput. Chem.* 31 (2010) 455-461.
- [19] A. Fais, B. Era, S. Asthana, V. Sogos, R. Medda, L. Santana, E. Uriarte, M.J. Matos, F. Delogu, A. Kumar, Coumarin derivatives as promising xanthine oxidase inhibitors, *Inter. J. Biolog. Macromol.* 120 (2018) 1286-1293.

- [20] M. Crawford, J.A.M. Shaw, Perkin coumarin synthesis, *J. Chem. Soc.* (1953) 3435-3439.
- [21] N.R. Krishnaswamy, T.R. Seshadri, B.R. Sharma, Nitro derivatives of 3-phenylcoumarins, *Ind. J. Chem.* 7(1) (1969) 49-55.
- [22] M.J. Matos, S. Vazquez-Rodriguez, L. Santana, E. Uriarte, C. Fuentes-Edfuf, Y. Santos, A. Munoz-Crego, Synthesis and structure-activity relationships of novel amino/nitro substituted 3-arylcoumarins as antibacterial agents, *Molecules* 18 (2013) 1394-1404.
- [23] J.F. Archer, J. Grimshaw, Electrochemical reactions. VI. Application of the Hammett relation to the polarographic reduction of substituted 9-benzylidenefluorenes and 3-phenylcoumarins, *J. Chem. Soc. [Section] B: Phys. Org.* 3 (1969) 266-270.
- [24] G. Ferino, E. Cadoni, M.J. Matos, E. Quezada, E. Uriarte, L. Santana, S. Vilar, N.P. Tatonetti, M. Yañez, D. Viña, C. Picciau, S. Serra, G. Delogu, MAO inhibitory activity of 2-arylbenzofurans versus 3-arylcoumarins : synthesis, in vitro study, and docking calculations, *ChemMedChem* 8 (2013) 956-966.
- [25] A. Bochicchio, L. Chiummiento, M. Funicello, M.T. Lopardo, P. Lupattelli, Efficient synthesis of 5-nitro-benzo[b]furans via 2-bromo-4-nitro-phenyl acetates, *Tetrahedron Lett.* 51 (2010) 2824-2827.
- [26] M.J. Bosiak, A convenient synthesis of 2-arylbenzo[b]furans from aryl halides and 2-halophenols by catalytic one-pot cascade method, *ACS Catal.* 6 (2016) 2429-2434.
- [27] H. Hao, W. Chen, J. Zhu, C. Lu, Y. Shen, Design and synthesis of 2-phenylnaphthale noids and 2-phenylbenzofuranoids as DNA topoisomerase inhibitors and antitumor agents, *Eur. J. Med. Chem.* 102 (2015) 277-287.
- [28] W. Pu, Y. Yuan, D. Lu, X. Wang, H. Liu, C. Wang, F. Wang, G. Zhang, 2-Phenylbenzo[b]furans: synthesis and promoting activity on estrogen biosynthesis, *Bioorg. Med. Chem. Lett.* 26 (2016) 5497-5500.
- [29] D.D. Qin, W. Chen, X. Tang, W. Yu, A.A. Wu, Y. Liao, H.B. Chen, Accessing 2-arylbenzofurans by CuI₂(pip)₂catalyzed tandem couplingcyclization reaction: mechanistic studies and application to the synthesis of stemofuran A and moracin M, *Asian J. Org. Chem.* 5 (2016) 1345-1352.

-
- [30] R. Arimboor, M. Rangan, S.G. Aravind, C. Arumugan, Tetrahydroamentoflavone (THA) from *Semecarpus anacardium* as a potent inhibitor of xanthine oxidase, *J. Ethnopharmacology* 133 (2011) 1117-1120.
- [31] A. Daina, O. Michielin, V. Zoete, SwissADME: a free web tool to evaluate pharmacokinetics, drug-likeness and medicinal chemistry friendliness of small molecules, *Sci. Rep.* 7 (2017) 42717.
- [32] Molinspiration Cheminformatics. Available online: <http://www.molinspiration.com/services/properties.html> (accessed on January 2020).



Allopurinol



Febuxostat

Figure 1

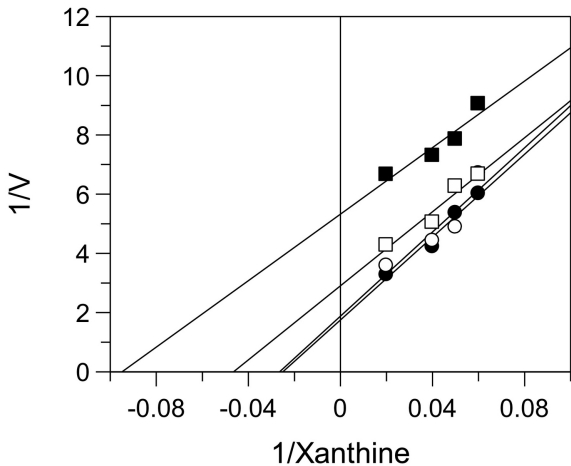


Figure 2

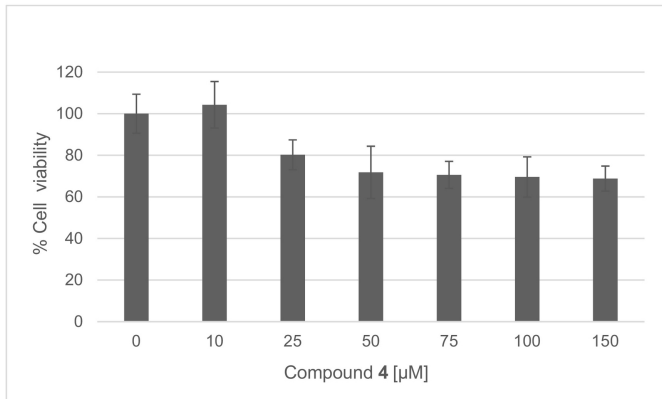


Figure 3

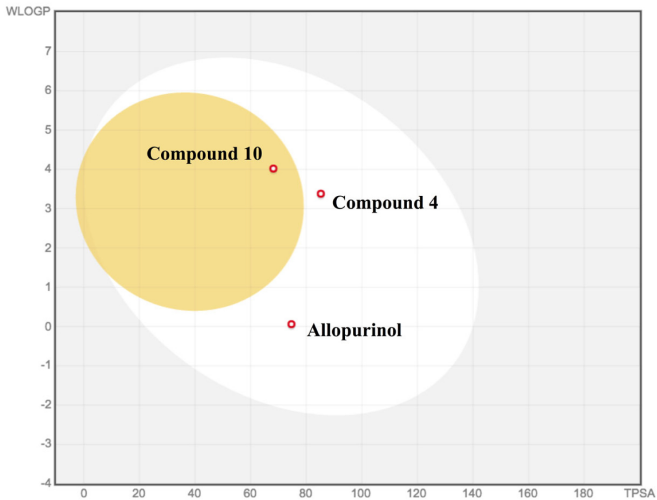


Figure 4

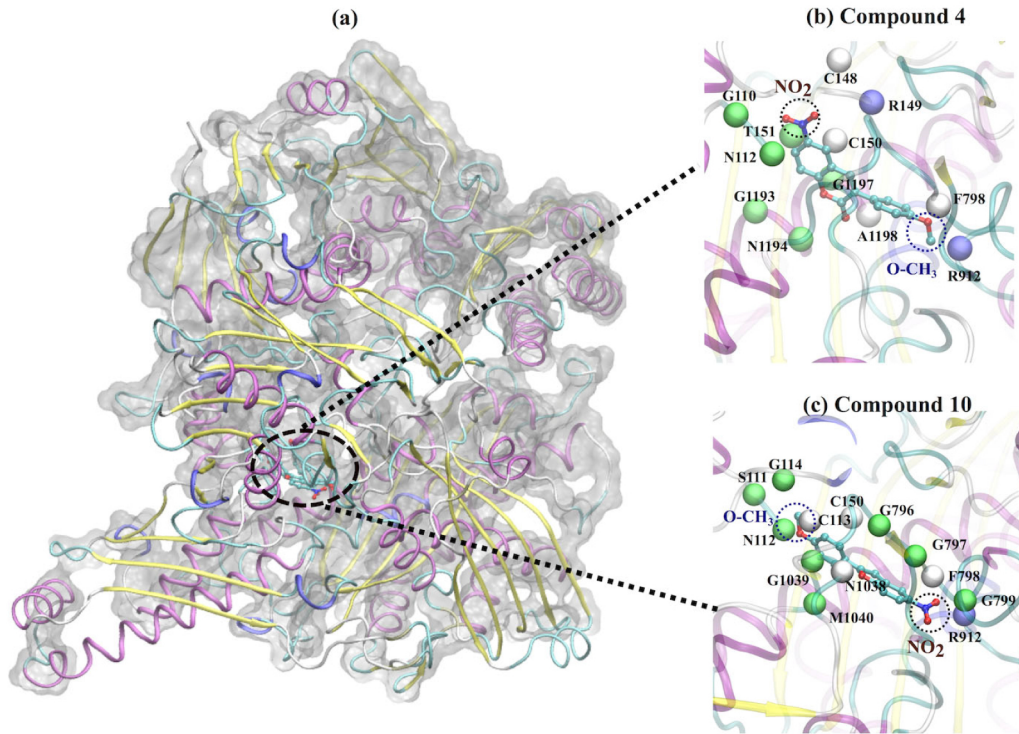
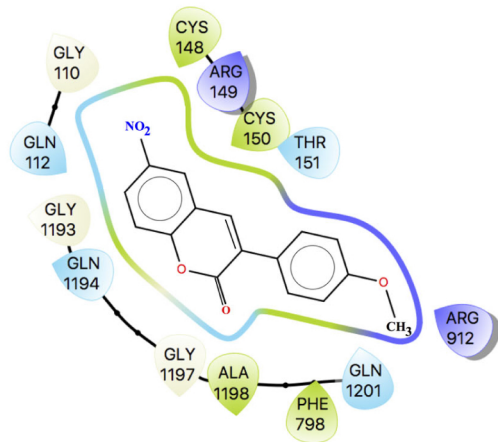


Figure 5

(a) Compound 4



(b) Compound 10

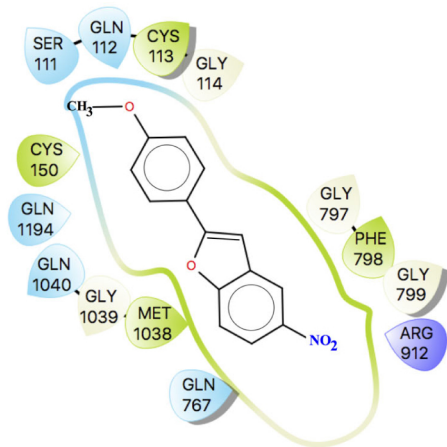


Figure 6